Original article

Changes in the Characteristics of Two-Phase Structure of Sea Ice under the Impact of Thermal Factors during the Period of its Growth

D. D. Zavyalov [⊠], T. A. Solomakha

Marine Hydrophysical Institute of RAS, Sevastopol, Russian Federation

□ zavyalov.dd@mhi-ras.ru

Abstract

Purpose. The study evaluates the impact of incorporating a two-phase ice structure into a thermodynamic model on its mechanical and thermophysical properties.

Methods and Results. The vertical distribution of thermophysical and physical-mechanical properties of sea ice was investigated using a model that assumes thermodynamic equilibrium between freshwater ice and brine (in solid and liquid phases). The heat transfer process is described by a nonlinear one-dimensional heat diffusion equation, excluding the effects of penetrating radiation and brine migration within the ice thickness. Salinity distribution was modeled using two approaches: an empirical relationship between bulk ice salinity and thickness, and a polynomial function reproducing the C-shaped vertical salinity profile typical of thin growing ice. Numerical experiments simulated the crystallization of brackish seawater under varying surface air temperatures, with and without accounting for the liquid phase in the ice cover. The results reveal the vertical distribution characteristics of thermophysical and physical-mechanical properties during ice growth.

Conclusions. The thermal conductivity of the upper ice layer is significantly lower when the two-phase structure is not considered, particularly during early ice formation. The permeability of ice formed from seawater with varying initial salinity and air temperatures was assessed. Time periods during which the upper ice layer of a specific thickness becomes impermeable to brine migration were determined.

Keywords: sea ice, sea ice growth, salinity, two-phase zone

Acknowledgements: The study was conducted as part of the state assignment of FSBSI FRC MHI FNNN-2021-0004 "Oceanological processes".

For citation: Zavyalov, D.D. and Solomakha, T.A., 2025. Changes in the Characteristics of Two-Phase Structure of Sea Ice under the Impact of Thermal Factors during the Period of its Growth. *Physical Oceanography*, 32(5), pp. 657-667.

© 2025, D. D. Zavyalov, T. A. Solomakha

© 2025, Physical Oceanography

Introduction

Sea ice cover consists of an aggregate of freshwater ice crystals, brine trapped within pores and gas bubbles. As salt dissolved in seawater is excluded from forming ice crystals, it is expelled into the brine solution between them. Sea ice is a two-phase porous medium, with its thermophysical properties determined by the combined characteristics of its liquid and solid phases. The internal structure and brine migration within the ice thickness influence its thermophysical, mechanical and optical properties, affecting mass and heat exchange between the ocean and atmosphere. Brine movement serves as the primary mechanism for biogeochemical processes within the ice cover and at the ice – sea water interface. The spatiotemporal variability of sea ice temperature and salinity, along with their influence on ice properties, enables the determination of the primary mechanical and

The content is smalled and a Constitution

ISSN 1573-160X PHYSICAL OCEANOGRAPHY VOL. 32 ISS. 5 (2025)

657

thermophysical characteristics of the ice cover, which are essential for addressing various scientific and practical challenges.

To investigate the internal structure of two-phase sea ice, accurate data on the vertical salinity distribution are required. The vertical salinity profile of sea ice evolves over time. During active growth, the salinity distribution exhibits a characteristic C-shaped profile. Subsequently, during the melting period, salinity decreases throughout the ice thickness, with the minimum value observed at the upper boundary 1 .

Climate models commonly employ thermodynamic sea ice packages, such as the Community Ice CodE (CICE) and the Louvain-la-Neuve Sea Ice Model (LIM). In the CICE model, salinity is treated as a prognostic variable [1], with gravitational drainage during the growth period parameterized as described in [2, 3]. In the LIM model [4, 5], only the mean salinity is predicted, while the vertical salinity profile is represented by a function of the mean salinity, which varies depending on the stage of sea ice development. A review of the historical development of models accounting for the spatiotemporal evolution of salinity and the porous structure of sea ice is provided in [6].

References [7, 8] describe a one-dimensional regional thermodynamic model of snow and sea ice cover, incorporating temporal changes in thickness-averaged ice salinity. The temperature profile is determined by solving a non-stationary heat conduction equation. The heterogeneity of the medium is accounted for by defining heat capacity and thermal conductivity as functions of sea ice temperature and salinity [9]. For reconstructing the seasonal dynamics of ice cover thickness, this approach is justified to some extent. The mechanical and thermophysical properties of sea ice, which govern its temperature profile, growth and melting, are highly dependent on salinity and temperature, particularly near the melting point, where the liquid phase volume undergoes significant changes. The challenge in parameterizing physical processes (brine migration, diffusion and gravitational drainage) that shape the sea ice salinity profile lies in their differing scales and the nonlinear relationship between salinity, ice structure, thickness and growth rate.

In this study, we implemented a parameterization of spatiotemporal salinity variation based on empirical data describing vertical salinity profile of growing first-year sea ice ¹. The proposed model does not explicitly resolve small-scale physical processes (brine migration and gravitational drainage); instead, their influence on the dynamics of salinity is taken into account indirectly through the determination of the characteristic vertical profile of sea ice salinity during the period of its growth. This approach enables the assessment of the variability of thermophysical and physical-mechanical properties of sea ice without requiring a significant reduction in the time step, which would otherwise complicate the implementation of the numerical scheme.

The model results for dynamic salinity were validated against data from a laboratory experiment simulating ice growth from a saline solution ². Vertical profiles of salinity, thermal conductivity and permeability (defined as a liquid phase

¹ Tsurikov, V.L., 1976. Liquid Phase in Sea Ice. Moscow: Nauka, 210 p. (in Russian).

² Notz, D., 2005. *Thermodynamic and Fluid-Dynamical Processes in Sea Ice*. Ph.D. Thesis. University of Cambridge, U.K., 222 p.

fraction greater than 5%) were determined for growing sea ice under various initial water salinity and surface air temperature conditions.

This study investigates the effect of incorporating a two-phase ice structure into a thermodynamic model on its mechanical and thermophysical properties.

Thermodynamic model

The thermodynamics of sea ice, incorporating a heterogeneous zone of mixed solid and liquid phases, is described by a nonlinear one-dimensional heat diffusion equation, excluding the effects of penetrating radiation and brine migration within the ice thickness, as presented in [6]:

$$(\rho c)_{m} \frac{\partial T}{\partial t} = \frac{\partial}{\partial z} \left(k_{m} \frac{\partial T}{\partial z} \right) + \rho_{i} L \frac{\partial \Phi}{\partial t}. \tag{1}$$

The boundary conditions at the upper (z = 0) and lower (z = h(t)) surfaces of the ice cover are defined by equations of heat and mass flux balance:

$$-k_{\rm m}\frac{\partial T}{\partial z} = F_{\rm t}(T_{\rm s}, T_{\rm a}), \quad -\rho_{\rm i}(1-\Phi)L_{\rm i}\frac{\partial h}{\partial t} = F_{\rm t}(T_{\rm 0}) + k_{\rm m}\frac{\partial T}{\partial z}, \quad z=0,$$
 (2)

$$-k_{\rm m}\frac{\partial T}{\partial z} = F_{\rm b}(T_{\rm f}, T_{\rm w}), \quad -\rho_{\rm i}(1-\Phi)L_{\rm i}\frac{\partial h}{\partial t} = F_{\rm b}(T_{\rm f}, T_{\rm w}) + k_{\rm m}\frac{\partial T}{\partial z}, \quad z = h(t), \tag{3}$$

where t is time; z is the vertical coordinate, the axis is directed downward from the upper surface of the ice cover (z=0); h is the ice thickness; ρ is density; T is temperature; c is specific heat; k is the thermal conductivity; S is salinity; L_i is latent heat of melting of fresh ice; Φ is the volume fraction of the solid phase; $L = \Phi(\rho_i c_i T - \rho_i L_i) - (1 - \Phi)\rho_{br} c_{br} T$ is the latent heat of melting of the two-phase zone; T_s , $F_t(T_s, T_a)$, T_f , $F_b(T_f, T_w)$ are the temperature and heat fluxes at the upper and lower ice boundaries; T_0 is the melting temperature of sea ice. In the absence of ice, the seawater temperature variation is determined by the balance of heat fluxes at the sea surface. The subscript m denotes the properties of the two-phase medium, calculated by the formula $X_m = \Phi X_i + (1 - \Phi) X_{br}$. Indices i, br, a, w refer to freshwater ice, brine, surface air layer and seawater, respectively.

The initial water temperature and salinity are specified as:

$$T_{\rm w}(z,0) = T_{\rm w0}, \quad S_{\rm w}(z,0) = S_{\rm w0}.$$
 (4)

The physical and thermophysical properties of freshwater ice and brine are determined as functions of temperature θ (°C) and salinity S (‰), as described in ²:

$$\rho_{i} = 917 - 0.1403 \cdot \theta, \quad \rho_{br} = 1000.3 + 0.78237 S_{br} + 2.8008 \cdot 10^{-4} S_{br}^{2},$$

$$k_{i} = 2.21 - 10^{-2} \cdot \theta + 3.44 \cdot 10^{-5} \cdot \theta^{2},$$

$$k_{\rm br} = 0.52325(1 - S_{\rm br} \cdot 10^{-3}) + 0.01256 \cdot \theta + 5.8604 \cdot 10^{-5} \cdot \theta^{2}, \tag{5}$$

$$c_{\rm i} = 2112.2 + 7.6973 \cdot \theta,$$

$$c_{\rm br} = 4208.8 + 111.71 \cdot \theta + 3.5611 \cdot \theta^{2} + 0.052168 \cdot \theta^{3},$$

$$L_{\rm i} = 333700 + 262.7 \cdot \theta - 7.929 \cdot \theta^{2}.$$

Thermodynamic equilibrium exists between freshwater ice and brine within salt pockets. The volume and salinity of brine inclusions are regulated to maintain the liquid phase at its freezing point (liquidus temperature). As sea ice cools, a portion of the brine freezes, increasing its salinity to preserve phase equilibrium. During ice melting, thermodynamic equilibrium is maintained by reducing brine salinity. Consequently, the brine salinity $S_{\rm br}$ is solely a function of temperature 2 $S_{\rm br} = -1.20 - 21.8 \cdot \theta - 0.919 \cdot \theta^2 - 0.0178 \cdot \theta^3$. For freshwater ice, $S_{\rm i} = 0$, the sea ice salinity is expressed as $S = (1 - \Phi)S_{\rm br}(\theta)$. The derived temperature and salinity distributions enable the determination of the temporal evolution of the phase composition and properties of sea ice.

In this study, sea ice salinity is not treated as a prognostic variable; instead, its spatiotemporal distribution is prescribed using the simulated salinity profile. For thin growing ice under calm weather conditions, a characteristic *C*-shaped vertical salinity profile persists for an extended period. During active sea ice growth, the salinity profile can be represented by a polynomial, as described in [10]:

$$S = S_{\text{max}}(0.981 - 1.482\eta + 3.741\eta^2 - 5.682\eta^3 + 3.362\eta^4), \ \eta = \frac{z}{h}, \tag{6}$$

where S_{max} is the sea ice salinity at the lower boundary, determined using empirical dependences of salinity on the rate of ice growth rate 1 [11] or ice thickness [12].

Numerical modeling results

The thermal regime of sea ice cover is modeled using a locally one-dimensional thermodynamic model. The vertical structure is represented by a fixed number of ice layers [7]. Solving equation (1) with boundary conditions (2), (3) and initial conditions (4) determines the heat propagation and vertical temperature profiles. The phase fraction Φ remains constant during each time step [3]. The growth rate, thickness and upper surface temperature of the sea ice are determined by the heat flux balance equations [7, 8]. Thermal conductivity, heat capacity and latent heat of melting of ice are expressed as empirical functions of temperature and salinity, as given in equations (5). Using the derived sea ice temperature and salinity profiles, the vertical distributions of solid and liquid phases, along with other physical properties, were calculated.

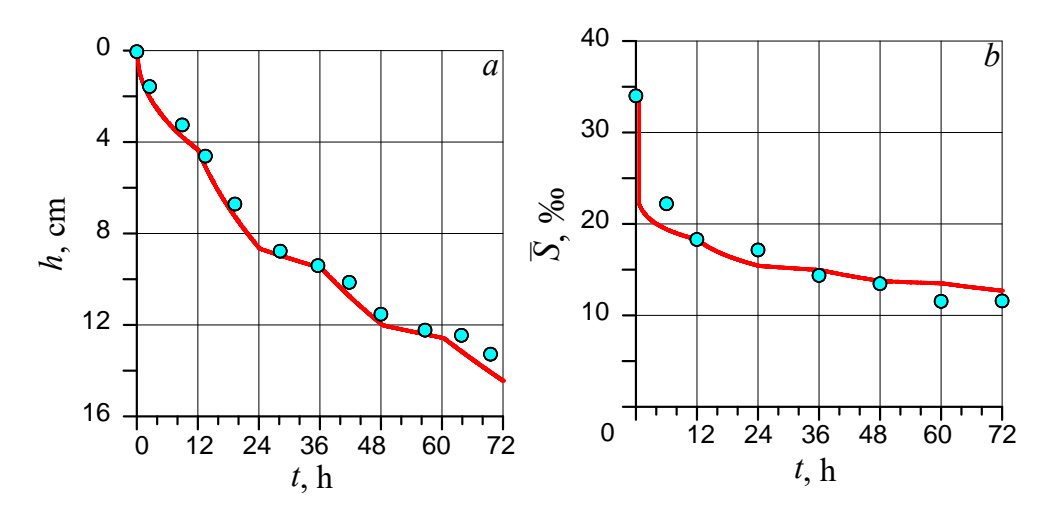
The numerical solution of equation (1) was obtained using the Crank-Nicolson scheme, with calculations performed for 30 ice layers and a time integration step of 30 s.

Model validation was conducted by comparing the results of test calculations with a laboratory experiment ² that measured the local solid fraction formed from a sodium chloride solution with a salinity of 34% during cooling from above.

The experiment lasted three days, with the surface ice temperature T_s alternating every 12 hours between -5 to -10 °C. Fig. 1 presents the modeled ice thickness and mean salinity, derived using the empirical relationship from [12]:

$$S(h) = S_{w} \left[(1-b) \exp(-a\sqrt{h}) + b \right]. \tag{7}$$

The best agreement between the laboratory data and modeling results was observed (Fig. 1) for the specified dependence (7) with fitted coefficient values a = 0.45; b = -2.5.



F i g. 1. Comparison of the calculated ice thickness (a) and average salinity (b) with the data of laboratory experiment ²: lines are calculation, circles are measurements

A series of numerical simulations was conducted to reconstruct the crystallization of brackish seawater using equation (6), where $S_{\rm max}$ was determined from equation (7), under periodic air temperature $T_{\rm a}$ variations between -5 to -10 °C every 12 hours for 5 days. The mechanical and thermophysical properties of sea ice were compared, considering both the presence and absence of a liquid phase within the ice thickness.

Vertical profiles of temperature, thermal conductivity and salinity for homogeneous (dashed lines) and heterogeneous (solid lines) sea ice under periodic air temperature variations are presented in Fig. 2. For the homogeneous ice model, the mean salinity is determined using equation (7) and the thermal conductivity is calculated using the formula $k = k_i + \frac{0.117S}{T}$ from [9].

The vertical profiles of temperature and thermal conductivity exhibit similar patterns in both models. The thermal conductivity decreases from the upper (ice – atmosphere) to the lower (ice – water) surface of the sea ice. In the homogeneous model, the thermal conductivity of the upper ice layer is significantly lower, particularly during early ice formation, compared to the heterogeneous model. However, for homogeneous ice formed from low-salinity water (Fig. 2, d), the vertical gradient and thermal conductivity near the lower boundary are higher

than in porous ice. Accounting for vertical salinity variability has a minor effect on the thickness of growing ice. For initial seawater salinities above 10%, the difference in ice thickness, calculated by different methods, does not exceed 3% (Fig. 2, b, e, h). However, for lower salinity, the differences are more pronounced (Fig. 2, a, d, g).

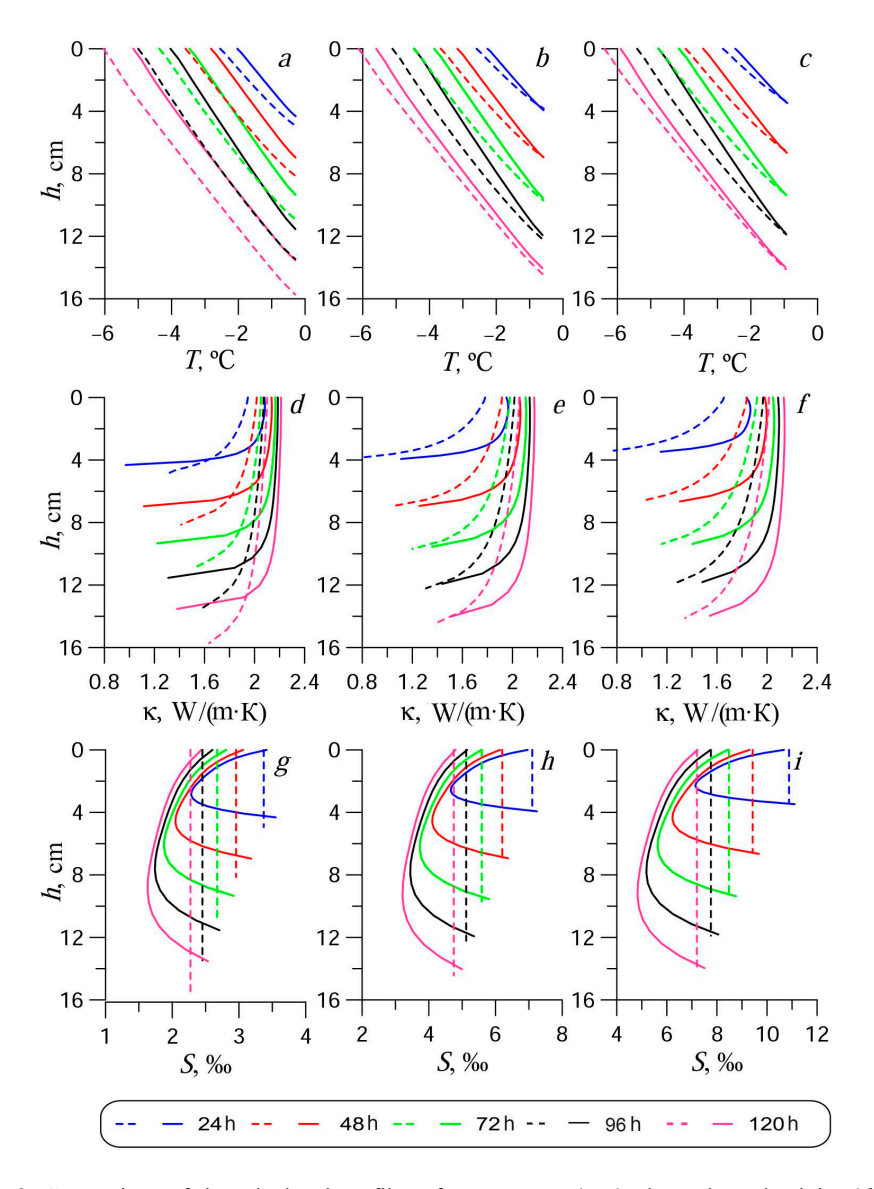
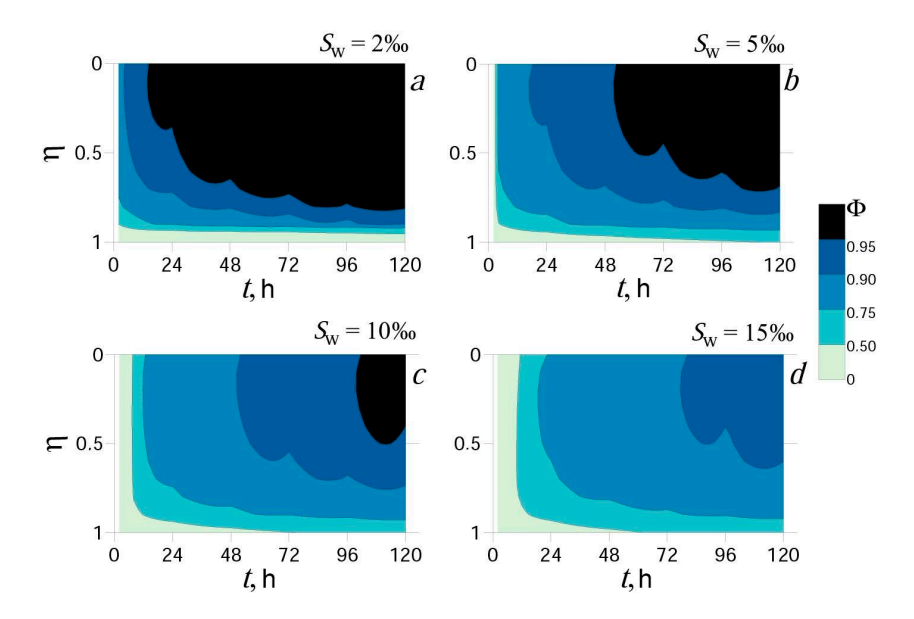


Fig. 2. Comparison of the calculated profiles of temperature (a-c), thermal conductivity (d-f) and salinity (g-i) for growing sea ice obtained with (solid lines) and without (dashed lines) regard to its two-phase structure. Fragments (a, d, g), (b, e, h) and (c, f, i) correspond to initial seawater salinities of 5, 10 and 15‰, respectively. Colors indicate duration of the time interval from the start of the experiment

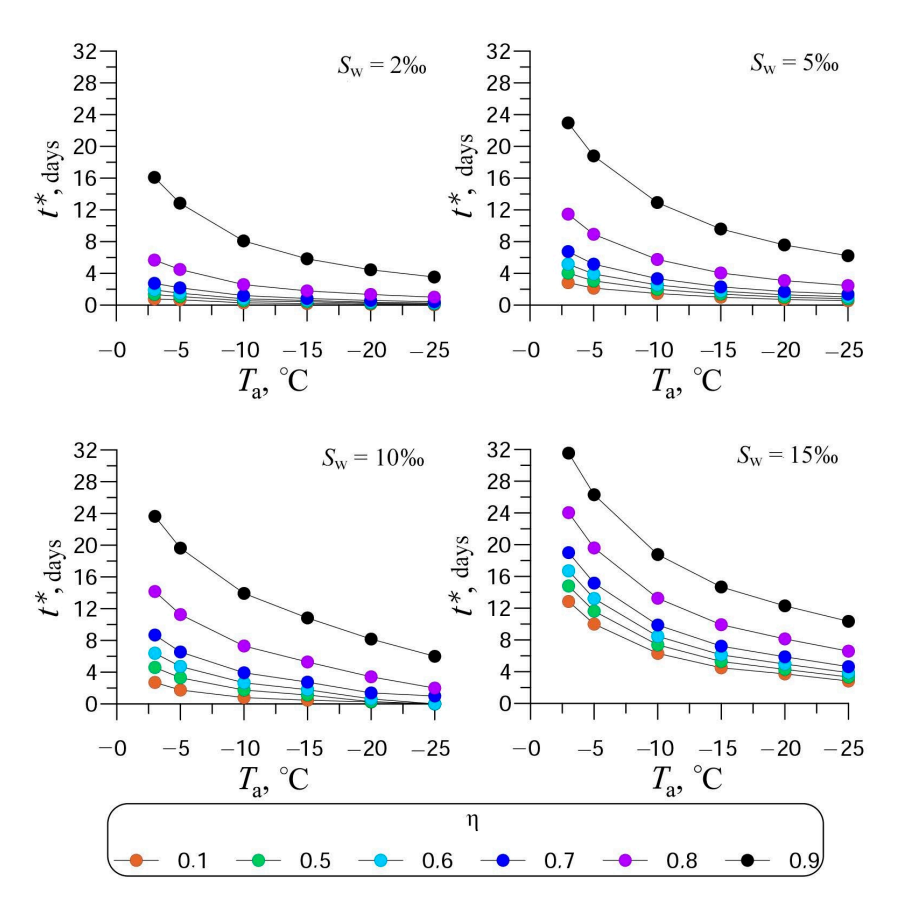
For the same temperature conditions, the permeability of the sea ice (defined as a liquid phase fraction greater than 5%) was assessed for varying initial seawater salinities. The solid phase fraction Φ relative to the dimensionless ice thickness η is presented in Fig. 3.

For a period following the onset of ice formation, the entire ice thickness remains permeable to vertical brine migration to some extent. The duration of this permeable period depends on both the initial seawater salinity and the surface air temperature $T_{\rm a}$. For ice formed from seawater with salinities of 2, 5 and 10‰, this period lasted approximately 14, 51 and 98 hours, respectively. Ice formed from seawater with a salinity of 15‰ remained permeable throughout its thickness by the end of the fifth day. Notably, brine migration in the bottom ice layer persisted throughout the experiment.

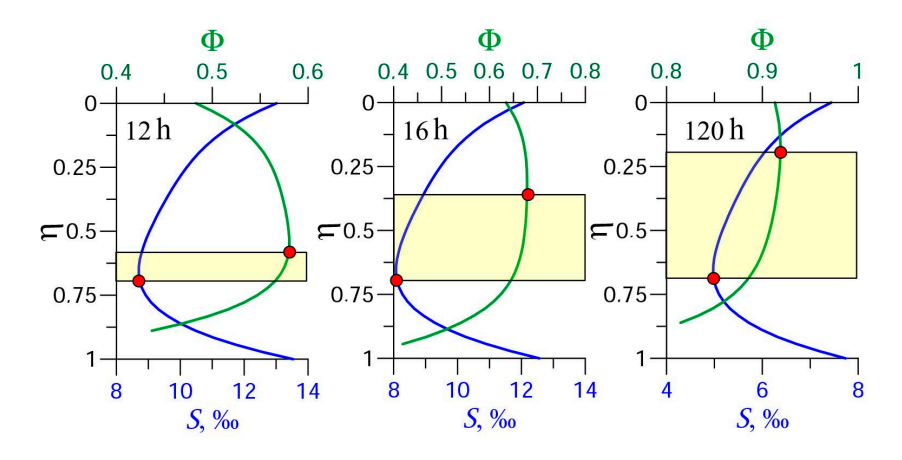


F i g. 3. Content of solid fraction Φ in sea ice relative to its dimensionless thickness under periodic changes in air temperature. Fragments (a), (b), (c) and (d) are given for the initial seawater salinities 2, 5, 10 and 15‰, respectively

For an experiment simulating sea surface cooling at constant air temperatures T_a of -3, -5, -10, -15, -20, -25 °C, with initial seawater salinities of 2, 5, 10, 15‰, the time intervals t^* during which the upper ice layer reaches a specified dimensionless thickness η and becomes impermeable were determined (Fig. 4). At lower temperatures, for the thickness of the upper impermeable layer within the range from $\eta = 0.1$ to $\eta = 0.7$, the curves are closely spaced. For example, with $S_w = 15‰$ and $T_a = -25$ °C, the difference in t^* between adjacent η values within this range does not exceed 20%. Significantly longer times are required for the ice to become impermeable at depths where $\eta > 0.7$. The time interval t^* for the solid phase fraction in the layer $0.7 \le \eta \le 0.9$ to reach a value of 0.95 is 2-8 times greater, depending on the ice formation conditions, than the time required for the onset of condition $\Phi \ge 0.95$ in the layer where $\eta < 0.7$.

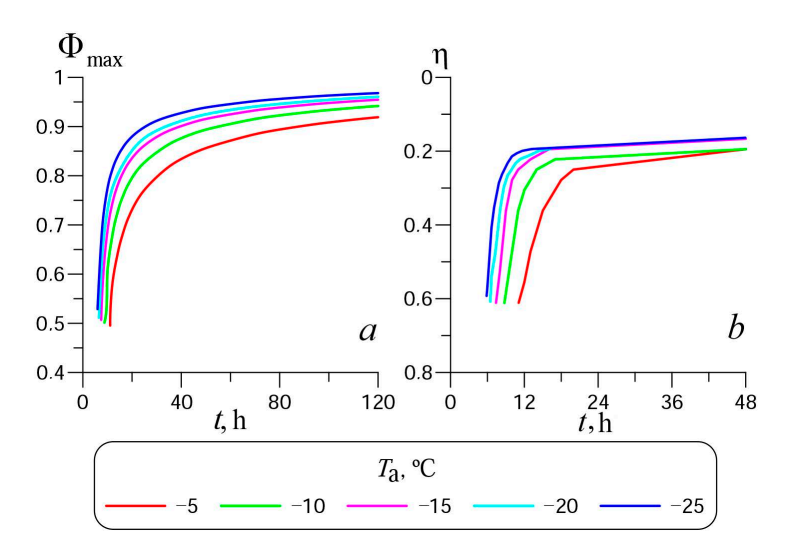


F i g. 4. Time from the onset of ice formation during which the top ice layer of a preset thickness becomes completely impermeable



F i g. 5. Relative position of the minimum salinity and the maximum content of solid phase of ice during the period of its growth at constant air temperature –5 °C and water salinity 15‰

Vertical profiles of salinity and solid phase fraction in sea ice exhibit extremum points during the growth period, as reported in [13, 14]. Fig. 5 illustrates the relative positions of the salinity minimum and the maximum solid phase fraction during ice growth at a constant air temperature $T_a = -5$ °C and an initial seawater salinity of 15%. Fig. 6 presents the maximum solid phase fraction (a) and the position (depth) of Φ_{max} within the ice (b) for various air temperatures.



F i g. 6. Maximum value of the solid phase (a) and position of Φ_{max} (b) during the period of ice growth

The salinity distribution used in the calculations, as described by equation (6), exhibits a minimum salinity at a depth of $\eta \approx 0.67$, with the position of the maximum solid phase fraction Φ_{max} varying over time. Based on the relative position of these extrema, the ice thickness can be divided into three distinct layers.

In the upper layer, decreasing salinity corresponds to an increasing solid phase fraction. In contrast, the lower layer shows increasing salinity, resulting in a decreasing solid phase fraction and an increasing brine content. The middle layer, situated between Φ_{max} and S_{min} , is characterized by a decrease in both salinity and solid phase fraction. At the onset of ice formation, Φ_{max} and S_{min} are closely positioned, minimizing the thickness of the middle layer, while the upper layer, where Φ increases, covers more than half of the total ice thickness. Over time, the value of Φ_{max} increases, and its position shifts toward the upper ice surface (Figs. 5, 6), leading to an expansion of the middle layer and a reduction in the upper layer, where Φ increases toward the lower ice surface. This shift may explain why the time required for the condition $\Phi \geq 0.95$ to be met in the layer below 0.7 h is significantly longer than for the layer above.

Conclusion

A numerical model of sea ice thermodynamics, accounting for its two-phase structure, has been developed. The primary physical-mechanical and thermophysical properties of sea ice were compared, considering both the presence and absence of a liquid phase within the ice thickness. The vertical profiles of thermal conductivity

exhibit similar patterns in both models. Thermal conductivity decreases from the upper (ice – atmosphere) to the lower (ice – water) surface of the sea ice. However, the thermal conductivity of the upper ice layer, obtained with no regard to the two-phase structure, turned out to be significantly lower, particularly during the early stages of ice formation.

A permeability assessment of sea ice formed from seawater with varying initial salinities and air temperatures is presented. Under periodic air temperature variations (from -5 to -10 °C every 12 hours), the entire ice thickness remains permeable to vertical brine migration for a period following the onset of ice formation. For ice formed from seawater with initial salinities of 2, 5, and 10‰, this permeable period lasted approximately 14, 51 and 98 hours, respectively. Ice formed from seawater with a salinity of 15‰ remained permeable throughout its thickness by the end of the fifth day. Notably, brine migration in the bottom ice layer persisted throughout the experiment.

For an experiment simulating sea surface cooling at constant air temperatures, the time intervals during which the upper ice layer reaches a specified thickness nand becomes impermeable were determined. Estimates of the maximum solid phase fraction Φ_{max} and its position within the ice during the growth period are provided. The relative positions of the salinity minimum and the maximum solid phase fraction are hypothesized to influence the time required for the ice to become impermeable.

REFERENCES

- Hunke, E.C., Hebert, D.A. and Lecomte, O., 2013. Level-Ice Melt Ponds in the Los Alamos Sea Ice Model, CICE. *Ocean Modelling*, 71, pp. 26-42. https://doi.org/10.1016/j.ocemod.2012.11.008
- Turner, A.K., Hunke, E.C. and Bitz, C.M., 2013. Two Modes of Sea-Ice Gravity Drainage: A Parameterization for Large-Scale Modeling. *Journal of Geophysical Research: Oceans*, 118(5), pp. 2279-2294. https://doi.org/10.1002/jgrc.20171
- 3. Turner, A.K. and Hunke, E.C., 2015. Impacts of a Mushy-Layer Thermodynamic Approach in Global Sea-Ice Simulations Using the CICE Sea-Ice Model. *Journal of Geophysical Research: Oceans*, 120(2), pp. 1253-1275. https://doi.org/10.1002/2014JC010358
- Vancoppenolle, M., Fichefet, T., Goosse, H., Bouillon, S., Madec, G. and Maqueda, M.A.M., 2009. Simulating the Mass Balance and Salinity of Arctic and Antarctic Sea Ice. 1. Model Description and Validation. *Ocean Modelling*, 27(1-2), pp. 33-53. https://doi.org/10.1016/j.ocemod.2008.10.005
- 5. Vancoppenolle, M., Fichefet, T. and Goosse, H., 2009. Simulating the Mass Balance and Salinity of Arctic and Antarctic Sea Ice. 2. Importance of Sea Ice Salinity Variations. *Ocean Modelling*, 27(1-2), pp. 54-69. https://doi.org/10.1016/j.ocemod.2008.11.003
- Hunke, E.C., Notz, D., Turner, A.K. and Vancoppenolle, M., 2011. The Multiphase Physics of Sea Ice: A Review for Model Developers. The Cryosphere, 5(4), pp. 989-1009. https://doi.org/10.5194/tc-5-989-2011
- 7. Zav'yalov, D.D. and Solomakha, T.A., 2021. Influence of Thermodynamic Model Resolution on the Simulation of Ice Thickness Evolution in the Sea of Azov. *Russian Meteorology and Hydrology*, 46(7), pp. 474-482. https://doi.org/10.3103/S1068373921070062
- 8. Zavyalov, D.D. and Solomakha, T.A., 2023. Features of Parameterizing Turbulent Interaction with Underlying Surface in the Regional Thermodynamic Model of Sea Ice. *Physical Oceanography*, 30(4), pp. 385-397.
- 9. Untersteiner, N., 1961. On the Mass and Heat Budget of Arctic Sea Ice. *Archiv für Meteorologie, Geophysik und Bioklimatologie, Serie A*, 12(2), pp. 151-182. https://doi.org/10.1007/BF02247491

- 10. Andreev, O.M. and Ivanov, B.V., 2007. Parameterization of First-Year Sea Ice Vertical Salinity Distribution for Problems of Thermodynamics Modeling in Arctic Regions. *Problemy Arktiki i Antarktiki*, 75(1), pp. 99-105 (in Russian).
- Petrich, C. and Eicken, H., 2009. Growth, Structure and Properties of Sea Ice. In: D. N. Thomas and G. S. Dieckmann, eds., 2009. Sea Ice. United Kingdom: Wiley-Blackwell, pp. 23-77. https://doi.org/10.1002/9781444317145.ch2
- 12. Ryvlin, A.Ya., 1974. [Method for Predicting the Ultimate Strength of the Ice Cover for Bending]. *Problemy Arktiki i Antarktiki*, 45, pp. 79-86 (in Russian).
- 13. Notz, D. and Worster, M.G., 2008. In Situ Measurements of the Evolution of Young Sea Ice. *Journal of Geophysical Research: Oceans*, 113(C3), C03001. https://doi.org/10.1029/2007JC004333
- Rees Jones, D.W. and Worster, M.G., 2014. A Physically Based Parameterization of Gravity Drainage for Sea-Ice Modeling. *Journal of Geophysical Research: Oceans*, 119(9), pp. 5599-5621. https://doi.org/10.1002/2013JC009296

Submitted 30.01.2025; approved after review 29.04.2025; accepted for publication 11.07.2025.

About the authors:

Dmitry D. Zavyalov, Senior Research Associate, arine Hydrophysical Institute of RAS (2 Kapitanskaya Str., Sevastopol, 299011, Russian Federation), CSc. (Phys.-Math.), **ORCID ID: 0000-0002-7444-980X**, **Scopus Author ID: 6506347014**, **ResearcherID: JUV-4477-2023**, zavyalov.dd@mhi-ras.ru

Tatyana A. Solomakha, Junior Research Associate, Marine Hydrophysical Institute of RAS (2 Kapitanskaya Str., Sevastopol, 299011, Russian Federation), ORCID ID: 0000-0001-5500-5763, Scopus Author ID: 8845393700, ResearcherID: JXL-7131-2024, solomaxa.ta@mhi-ras.ru

Contribution of the co-authors:

Dmitry D. Zavyalov – development of the research methodology, creation of the software module, conducting numerical experiments, analysis and visualization of research results, writing and editing of the manuscript

Tatyana A. Solomakha – collection and analysis of scientific literature, development of algorithms for the software module, writing and editing of the manuscript

The authors have read and approved the final manuscript. The authors declare that they have no conflict of interest.